geosciences

MDPI

Article

Effect of Moisture Content on Subgrade Soils Resilient Modulus for Predicting Pavement Rutting

Md Mostaqur Rahman [1], Sarah L. Gassman [2] and Kazi Moinul Islam [2,*]

[1] Virginia Department of Transportation, 1700 N Main St., Suffolk, VA 23434, USA; mostaqur.rahman@vdot.virginia.gov

[2] Department of Civil and Environmental Engineering, University of South Carolina, 300 Main St., Columbia, SC 29208, USA

* Correspondence: kislam@email.sc.edu; Tel.: +1-803-360-3836

Abstract: The subgrade soil stiffness, which depends on the in-situ moisture content and soil index characteristics, is a key factor in pavement rutting. Due to variations in the compaction process used during construction and seasonal changes, the subgrade soil moisture content may deviate from the desired condition. The resilient modulus (M_R), an important parameter of the Mechanistic-Empirical (M-E) pavement design process, is used to specify the subgrade soil stiffness. Repeated load triaxial tests, which can be challenging and time-consuming to execute, are often used to determine M_R. As a result, correlations between M_R and more accessible stiffness metrics and index qualities are frequently used. California bearing ratio (CBR) and repeated load triaxial tests were carried out in this investigation. Soil specimens were fabricated at moisture levels that were both above and below the optimum moisture content (w_{opt}). The results of the two tests were correlated, and statistical models were created to correlate the parameters of the generalized constitutive resilient modulus model with the characteristics of the soil index. Additionally, utilizing the M_R found for subgrade soils compacted at w_{opt} and $\pm 2\% w_{opt}$, pavement rutting was analyzed for three base layer types. The results demonstrated that a laboratory-measured M_R ($M_{R(Lab)}$) decreases as the moisture content increases. Specimens compacted at $-2\% w_{opt}$ showed higher $M_{R(Lab)}$ than specimens compacted at w_{opt}. Specimens compacted at $+2\% w_{opt}$ showed lower $M_{R(Lab)}$ than specimens compacted at w_{opt}. Results also indicated that the $M_{R(Lab)}$ predicted higher pavement rutting compared to field measured M_R ($M_{R(Lab)}$). If a stabilized aggregate foundation layer was employed instead of an untreated granular base, subgrade soil moisture condition showed a significant impact on rutting.

Keywords: resilient modulus; moisture content; CBR; pavement rutting

check for updates

Citation: Rahman, M.M.; Gassman, S.L.; Islam, K.M. Effect of Moisture Content on Subgrade Soils Resilient Modulus for Predicting Pavement Rutting. *Geosciences* **2023**, *13*, 103. https://doi.org/10.3390/geosciences13040103

Academic Editors: Jesus Martinez-Frias and Mohamed Shahin

Received: 8 February 2023
Revised: 22 March 2023
Accepted: 28 March 2023
Published: 30 March 2023

1. Introduction

Rutting is a structural distress that affects the riding quality and structural performance of flexible pavements. The structural life of a pavement is affected by several factors, including traffic conditions [1,2], climatic conditions [3,4], and pavement and subgrade materials [5–8]. To predict distresses, such as pavement rutting and roughness, over the design life of the pavement, the Mechanistic-Empirical Pavement Design Guide (MEDPG) [9] is used. The subgrade resilient modulus (M_R), out of all the material inputs, has been determined to have the most significant influence on rutting predicted by MEPDG [10,11]. A repeated load triaxial (RLT) test can be used to directly obtain M_R, although the test is considered difficult, time-consuming, and expensive. As a result, correlations of M_R to other parameters are frequently used. These include correlations to the pavement resilient modulus found using the falling weight deflectometer (FWD) (e.g., refs. [12–17]) and correlations to the dynamic cone penetrometer [18] and California Bearing Ratio (CBR) (e.g., refs. [19–21]). Additionally, correlations between M_R from RLT tests and soil index properties have been developed (e.g., refs. [22–26]). Instead of covering a range of moisture conditions and dry densities, most correlations are for a specific subgrade condition, such as the optimum moisture condition and maximum dry density. Moisture variation significantly influences subgrade M_R and, subsequently, pavement performance [25,27–30]. Soil samples compacted on the wet side of w_{opt} have been shown to experience higher permanent strain potentials than those compacted dry side of w_{opt} and at w_{opt} [31]. An increase in moisture content above optimum has decreased M_R. However, M_R results obtained for specimens on the dry side were close to those of samples tested at w_{opt} [30]. Subgrade M_R also varies seasonally because of changes in moisture content [28].

In recent years, there has been an increased interest in determining the effect of moisture changes on the mechanical behavior of subgrade soils [32–35]. The new MEPDG stresses the importance of these environmental conditions. It incorporates them in pavement design through models that analyze the changes in mechanical properties with moisture variations. The soil water characteristics curve is used to evaluate seasonal changes in moisture contents and to define the relationship between the variations of water contents with soil suction in unsaturated subgrade soil. Resilient modulus is sensitive to moisture changes and the state of stresses dictated by the soil suction within a subgrade layer. Knowledge of moisture impact and suction's influence on the subgrade's resilient modulus is necessary when designing and rehabilitating new pavements [36].

Since there have been few studies on the effects of moisture variation of subgrade M_R on pavement rutting in MEPDG (e.g., ref. [25]) and few studies on the correlations between M_R and soil index properties and alternate stiffness test parameters for a range of moisture contents, e.g., refs. [23,25,29], the goal of this study is to conduct RLT tests and CBR tests on specimens at various moisture contents and establish relations between the results to predict M_R and subsequent pavement rutting for moisture concentrations at, above, and below w_{opt} using MEPDG. Finally, the influence of subgrade soil moisture content on resilient modulus and pavement rutting will be investigated for three commonly used base types in South Carolina.

2. Objectives

The main research question addressed in this study is How does moisture content affect the subgrade M_R for predicting pavement rutting using MEPDG? The primary research hypothesis associated with this research question is that M_R can be effectively used as an appropriate design input parameter for MEPDG in efforts to simulate different moisture conditions.

The following research tasks were completed in an effort to answer the research question:

1. Perform repeated load triaxial tests on remolded samples of subgrade soil collected from beneath existing pavements. Determine M_R of these subgrade soils at different moisture contents above and below the optimum moisture content.
2. Conduct CBR tests on specimens remolded at different moisture contents and densities.
3. Develop a correlation between CBR and the resilient modulus from repeated load triaxial tests. Establish statistical models between soil index properties and the resilient modulus model parameters for remolded soils.
4. Back-calculate $M_{R(FWD)}$ from FWD tests performed on existing pavements where the subgrade soil samples were obtained. Relate the laboratory-measured $M_{R(Lab)}$ to the back-calculated $M_{R(FWD)}$ and obtain the coefficient of conversion (C-factor).
5. Evaluate the effect of subgrade resilient modulus obtained for a range of moisture contents and densities on pavement rutting using the MEPDG software v2.6.1 for different pavement base types.

3. Methodology

Eight different subgrade soils were selected for this study. Soil samples were collected at 25 locations from beneath three existing pavement sections in different South Carolina regions. Pavement A is a 6.5-km section of US-521 in Georgetown County, Pavement B is a 9.9 km section of US-321 in Orangeburg County, and Pavement C is a 2.1 km section of SC-93 in Pickens County. Asphalt cores of 152.4 mm diameter were collected from the center of the right lane at spacings of 457 to 914 m along each pavement section. Samples of the subgrade soil were taken from beneath the asphalt core. There were 7 boreholes along Pavement A, 13 along Pavement B, and 5 along Pavement C. Approximately 22.6 kg of bulk soil was retrieved from each borehole, which was used for M_R, CBR, and geotechnical index tests. Shelby tube samples were obtained in addition to the bulk samples.

Soils were classified according to both USCS (ASTM D2488) and AASHTO (AASHTO M145). Soils were compacted in a standard Proctor mold (101.6 mm in diameter and 116.4 mm in height, compacted in three layers, 25 blows per layer) and a CBR mold (152.4 mm in diameter and 177.8 mm in height, compacted in three layers, 56 blows per layer) to establish relationships between density and moisture content. The relations were compared to the moisture and density of the field samples to show how well the laboratory-prepared samples represented the field conditions for different soil types.

CBR tests were performed by AASHTO T 193 [37]. Specimens were prepared at moisture contents of w_{opt}, $\pm 4\% w_{opt}$, $\pm 2\% w_{opt}$, and others as needed to define the relation between CBR and moisture content. CBR values were calculated as the ratio of load needed for 2.54 mm penetration of a circular spindle of 1935 mm^2 in the area to 1360 kg load or for 5.08 mm penetration to 2041 kg load.

Repeated load triaxial tests were performed as per AASHTO T307 [38]. Specimens were fabricated by compacting the soil in a CBR mold at moisture contents of $\pm\%2 w_{opt}$ and w_{opt}. Once the soil was compacted in the CBR mold, a 76.2 mm diameter Shelby tube was pushed into the soil to collect a 76.2 mm diameter $\times$ 152.4 mm long cylindrical specimen. The specimen was then extruded, inserted into a rubber membrane, and subjected to static confining pressure. A repeated axial cyclic stress of fixed magnitude, load duration, and cycle duration was applied per the testing sequence in AASHTO T307 [38].

The generalized constitutive resilient modulus model and Equation (1) was used to determine M_R from laboratory testing [39]:

$$M_R = k_1 P_a \left[\frac{\sigma_b}{P_a}\right]^{k_2} \left[\frac{\tau_{oct}}{P_a} + 1\right]^{k_3} \tag{1}$$

where P_a is atmospheric pressure, σ_b is bulk stress = $\sigma_1 + \sigma_2 + \sigma_3$, σ_1 is major principal stress, σ_2 is intermediate principal stress, σ_3 is minor principal stress, τ_{oct} is octahedral shear stress, and k_1, k_2, and k_3 are model parameters/material constants, was used to calculate the $M_{R(Lab)}$ with a confining stress (σ_3) equal to 13.8 kPa, and cyclic stress (deviator) stress equal to (σ_d) 41.4 kPa per NCHRP-285 [39].

Equation (2) [9] was used to estimate M_R from CBR and serve as a comparison to the M_R vs. CBR relation developed in this study.

$$M_R(\text{MPa}) = 17.6 \times \text{CBR}^{0.64} \tag{2}$$

FWD tests were performed at intervals of about 61 m along the three pavement sections. There were 80 stations along Pavement A, 155 along Pavement B, and 36 stations along Pavement C. The Dynatest system was used to conduct the FWD testing [40]. The device has 7 sensors with 7 distinct offsets (0, 203, 305, 457, 610, 915, and 1194 mm from the loading plate). Impulse loads of 4 different magnitudes (30.5, 40, 54, and 70 kN) were used for each test. Deflection basin data were collected and used to evaluate the pavement's condition and estimate the backcalculated modulus, $M_{R(FWD)}$, using the AASHTOWare backcalculation tool [41].

The effect of M_R on pavement rutting using the MEPDG was studied for five different resilient modulus input types: backcalculated from FWD data ($M_{R(FWD)}$), M_R obtained from 2% dry side of w_{opt} ($M_{R(Lab,\ Dry)}$), w_{opt}($M_{R(Lab,\ w_{opt})}$) 2% wet side of w_{opt}($M_{R(Lab,\ Wet)}$), and using the PMED default value based on soils classification ($M_{R(Default)}$). The default resilient modulus value was obtained for the unbound materials based on correlations to the soil classification in the MEPDG [3]. The value of 110 MPa, 124 MPa, and 90 MPa was used for Site A, Site B, and Site B, respectively. A summary of the MEPDG inputs is shown in Table 1. Pavement A, Pavement B, and Pavement C are asphalt concrete pavements with different bases [42]. Pavement A has a cement-stabilized base, Pavement B has a graded aggregate base, and Pavement C has an asphalt aggregate base. The construction dates for Pavement A, Pavement B, and Pavement C pavement sections are 2003, 2004, and 2001, respectively. The MEPDG analysis was run for 20 years.

Table 1. Summary of MEPDG Inputs.

County.		Pavement A	Pavement B	Pavement C
Base Year AADTT		368	720	490
AC Layer and Thickness (mm)		PG 76-22 (96.5)	PG 76-22 (142.2)	PG 76-22 (86.3)
Effective Binder Content (%)			11.6	
Air Void (%)			7	
Base Layer and Thickness (mm)		Cement Stabilized (152.2)	Graded Aggregate (152.2)	Asphalt Aggregate (147.3)
Base Elastic Modulus, MPa		6894	138	6894
Subgrade Layer and Thickness (mm)		A-3 (semi-infinite)	A-2-4 (semi-infinite)	A-7-6 (semi-infinite)
Subgrade Resilient Modulus, MPa	$M_{R\ (Lab,\ Dry)}$ [1]	114	112	107
	$M_{R\ (Lab,\ w_{opt})}$ [1]	96	77	84
	$M_{R\ (Lab,\ Wet)}$ [1]	76	45	38
	$M_{R\ (FWD)}$ [2]	310	361	190
	$M_{R\ (Default)}$ [3]	110	124	90

Note: [1] Average M_R for each site found from repeated load triaxial tests per AASHTO T93 on a remolded sample at 2% dry side of w_{opt}, w_{opt}, 2% wet side of w_{opt}. [2] Average back-calculated M_R for each site found from FWD tests using the AASHTOWare back-calculation tool (v 1.1.2) [41]. [3] Directly taken from PMED software latest version 2.6.1. For this study, $\beta_{s_1} = \beta_{GB}$ = 2.979 for unbound untreated/stabilized granular base; $\beta_{s_1} = \beta_{SG} = 0.393$ for subgrade material;$\beta_{r_1} = 0.24$, $\beta_{r_2} = 1$, $\beta_{r_3} = 1$ for asphalt concrete layer. Studies are ongoing to develop the final local calibration coefficients for South Carolina.

4. Results

4.1. Index Test Results

The properties of the investigated soils are shown in Table 2. The samples listed represent one sample for each of the eight different soil classifications (considering both USCS and AASHTO) found at the pavement sites. The soil samples from all Pavement A and Pavement B boreholes were classified as coarse-grained soils. Fine-grained soil is defined as having more than 50% passing the No. 200 sieve per USCS and 35% per AASHTO. Using the AASHTO criteria, Pavement C is fine-grained soil.

Table 2. Properties of Investigated Soils.

Site	Bore-Hole No.	Passing No. 200 Sieve (%)	wL (%)	wP (%)	PI (%)	G_s	w_{opt} (%)	$\gamma_{d,\ max}$ (kN/m^3)	Soil Classification	
									USCS	AASHTO
Pavement A	A-1	1.5	NP	NP	NP	2.65	9.3	19.5	SP	A-1-b
	A-4	0.8	NP	NP	NP	2.71	12.2	17	SP	A-3
Pavement B	B-3	24.7	26	17	9	2.66	10.1	19.8	SC	A-2-4
	B-6	20.6	18	17	1	2.39	10.7	19.4	SM	A-2-4
	B-8	22.8	20	16	4	2.6	10.6	19.5	SC-SM	A-2-4
Pavement C	C-2	43.8	45	29	16	2.55	15.1	17.6	SM	A-7-6
	C-4	51.2	36	26	10	2.52	16.3	17.7	ML	A-4
	C-5	44	42	28	14	2.51	13.8	18.5	SC	A-7-6

Note: wL = liquid limit, wP = plastic limit, PI = plasticity index, G_s = specific gravity of soil, w_{opt} = optimum moisture content, $\gamma_{d,\ max}$ = maximum dry unit weight, NP = Non-plastic.

Relationships between γ_d and moisture content developed for specimens compacted in a standard Proctor mold and a CBR mold are shown in Figure 1. Samples compacted in the CBR molds had $\gamma_{d,\ max}$ and w_{opt} close to that of the samples compacted in the Proctor mold. Field moisture content and dry density found from Shelby tube samples are also shown. The dry unit weights for the field samples were 3–22% less than the standard Proctor dry density, except for the Pavement C C-4 field samples, which were 4% lower to 9% higher than obtained from the standard Proctor test.

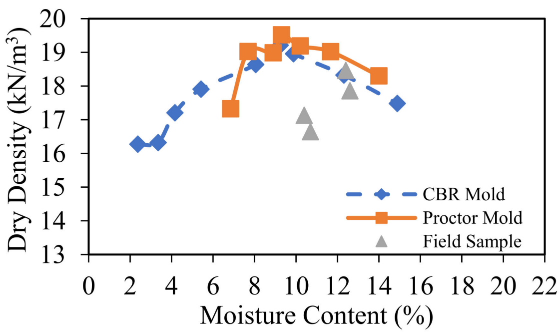

(**a**) Pavement A A-1 (SP/A-1-b)

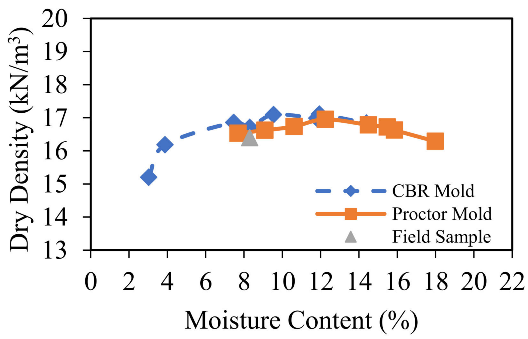

(**b**) Pavement A A-4 (SP/A-3)

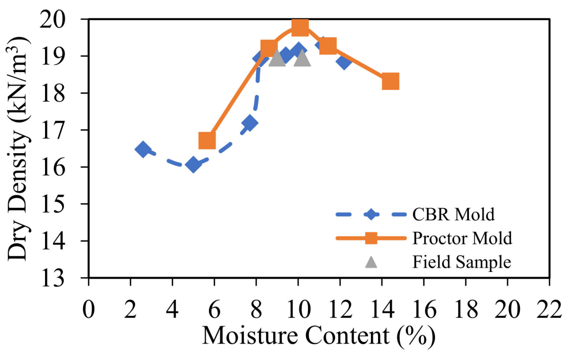

(**c**) Pavement B B-3 (SC/A-2-4)

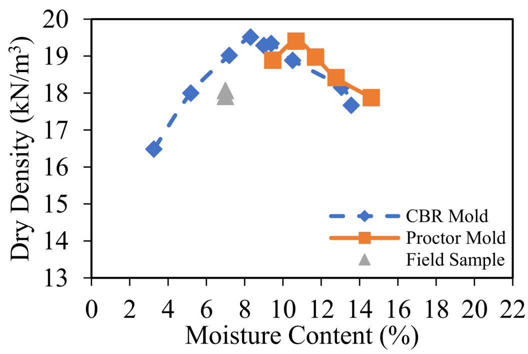

(**d**) Pavement B B-6 (SM/A-2-4)

Figure 1. *Cont.*

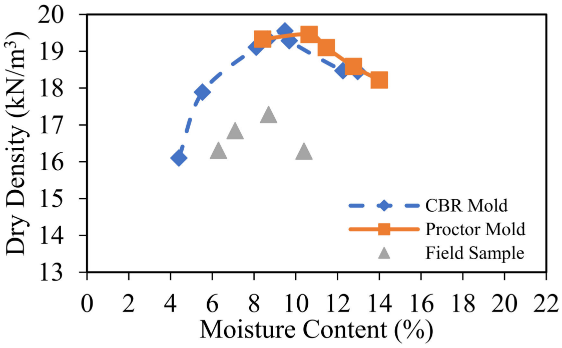

(**e**) Pavement B B-8 (SC-SM/A-2-4)

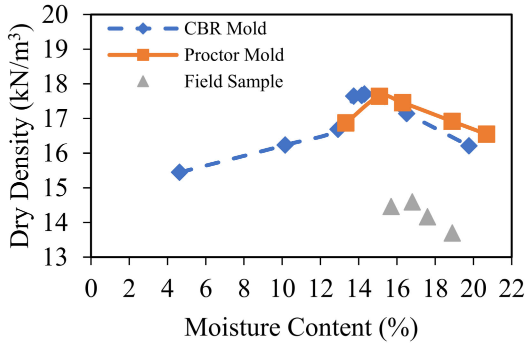

(**f**) Pavement C C-2 (SM/A-7-6)

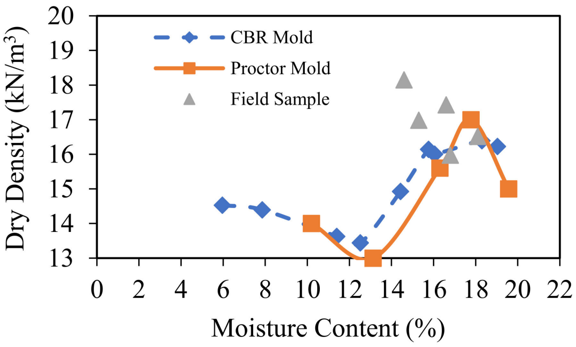

(**g**) Pavement C C-4 (ML/A-4)

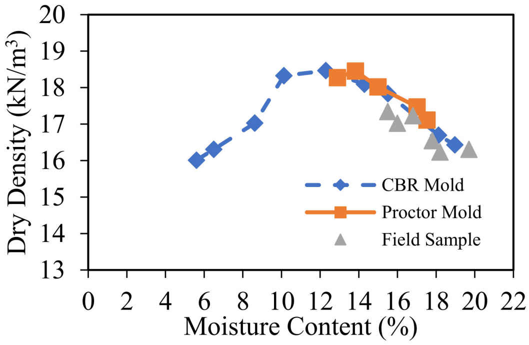

(**h**) Pavement C C-5 (SC/A-7-6)

Figure 1. Relationships between Density and Moisture Content.

4.2. CBR Test Results

The CBR results for penetration depths of 2.54 mm and 5.08 mm over a range of moisture contents are shown in Figure 2. For all eight soils, the CBR and moisture content relationships show a distinct peak similar to the moisture–density relation found from a standard Proctor compaction test (i.e., Figure 1). For the penetration of 2.54 mm, the peak CBR values were found to be 31 and 17 for Pavement A A-1 and A-4, respectively; 25, 18, and 28 for Pavement B B-3, B-6, and B-8, respectively; and 16, 18, and 21 for Pavement C C-2, C-4, and C-5, respectively. The peak CBR for penetration of 5.08 mm was 8% to 25% higher than the peak CBR for penetration of 2.54 mm for the Pavement B soils, 11% to 83% higher than the peak CBR for Pavement A soils, and about the same for the Pavement A soils. Note that the peak value of CBR does not coincide with the w_{opt}. Instead, it is on the dry side of optimum (0.5% to 5% dry side for the different soils).

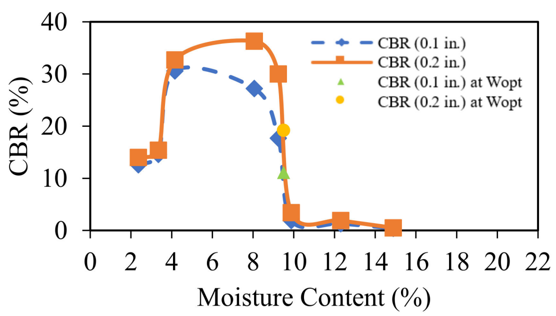

(a) Pavement A A-1 (SP/A-1-b)

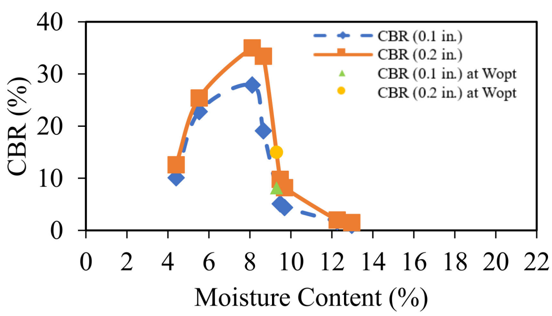

(b) Pavement A A-4 (SP/A-3)

Figure 2. *Cont.*

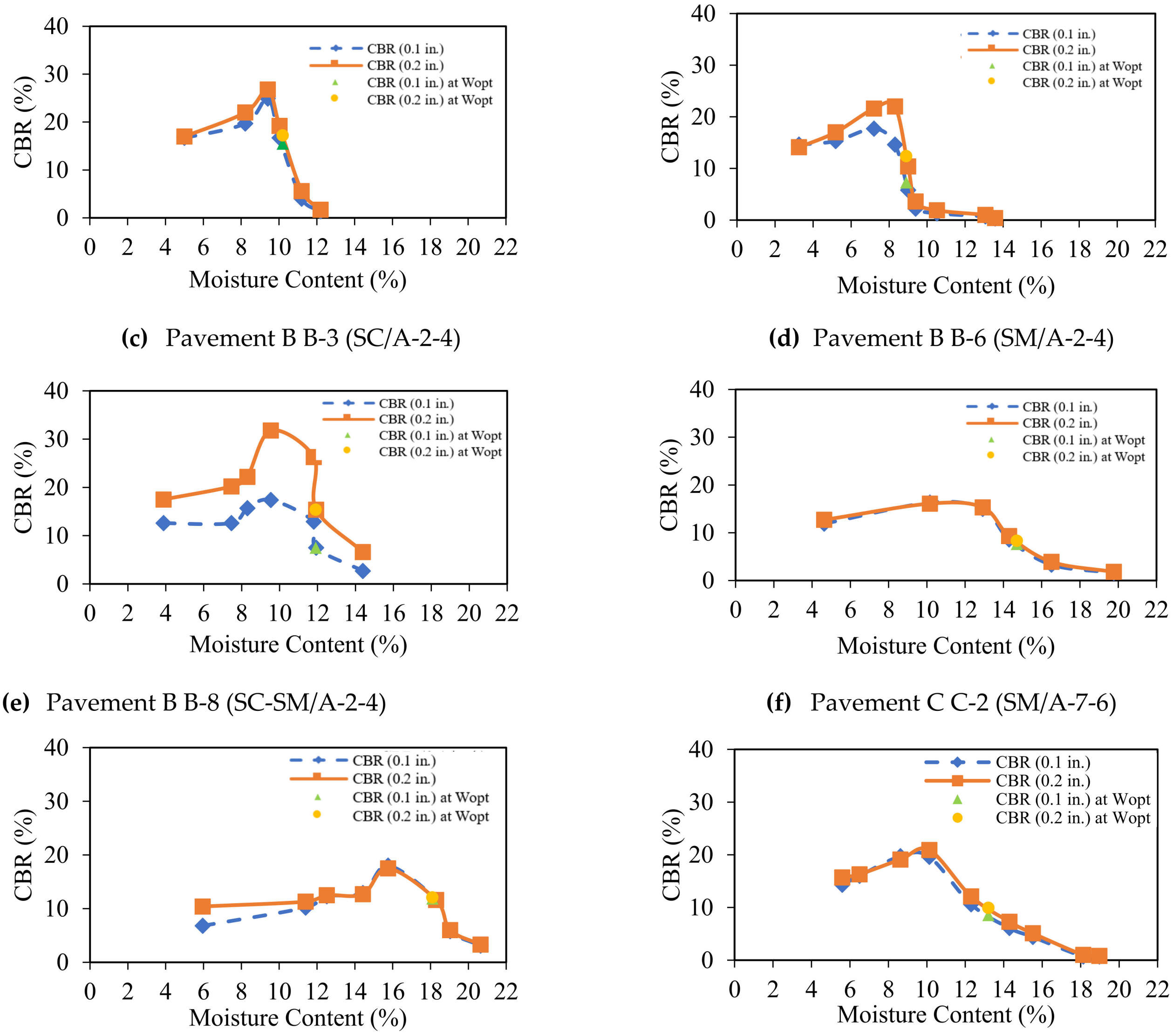

(c) Pavement B B-3 (SC/A-2-4)

(d) Pavement B B-6 (SM/A-2-4)

(e) Pavement B B-8 (SC-SM/A-2-4)

(f) Pavement C C-2 (SM/A-7-6)

(g) Pavement C C-4 (ML/A-4)

(h) Pavement C C-5 (SC/A-7-6)

Figure 2. CBR With Moisture Content.

4.3. Resilient Modulus Results

M_R test results for Pavement A A-1, Pavement B B-6, and Pavement C C-4 are shown in Figure 3 to illustrate results for each of the three sites. M_R versus cyclic stress at three different confining pressures is shown for specimens prepared at $-2\%w_{opt}$, w_{opt}, and $+2\%w_{opt}$. For the two granular soils (Pavement A in Figure 3a,b and Pavement B in Figure 3c–e), M_R increases with increasing cyclic stress, and a higher M_R is found for higher confining pressure, whereas, for the finer-grained soil (Pavement C in Figure 3f–i), M_R decreases with increasing cyclic stress. These trends agree with published literature (i.e., refs. [15,43–47]) illustrating the strain-hardening effect in sands and the stress-softening effect in clays. The softening effect decreases the resilient modulus of cohesive soils with increased deviator stress. Cohesive soils, if typically consolidated, soften while sheared and remolded. A decrease in stress is observed at strains beyond the peak stress; therefore, resilient modulus decreases. For loose granular soils, the resilient modulus increases with an increase in deviator stress, which indicates strain hardening (granular interlock) due to particle reorientation into the denser state [42]. Research studies have shown that subgrade M_R decreases with an increase in moisture content or degree of saturation [42–48]. Butalia et al. [49] observed a reduction in resilient modulus due to increased positive pore pressure with increased moisture content for unsaturated cohesive soils.

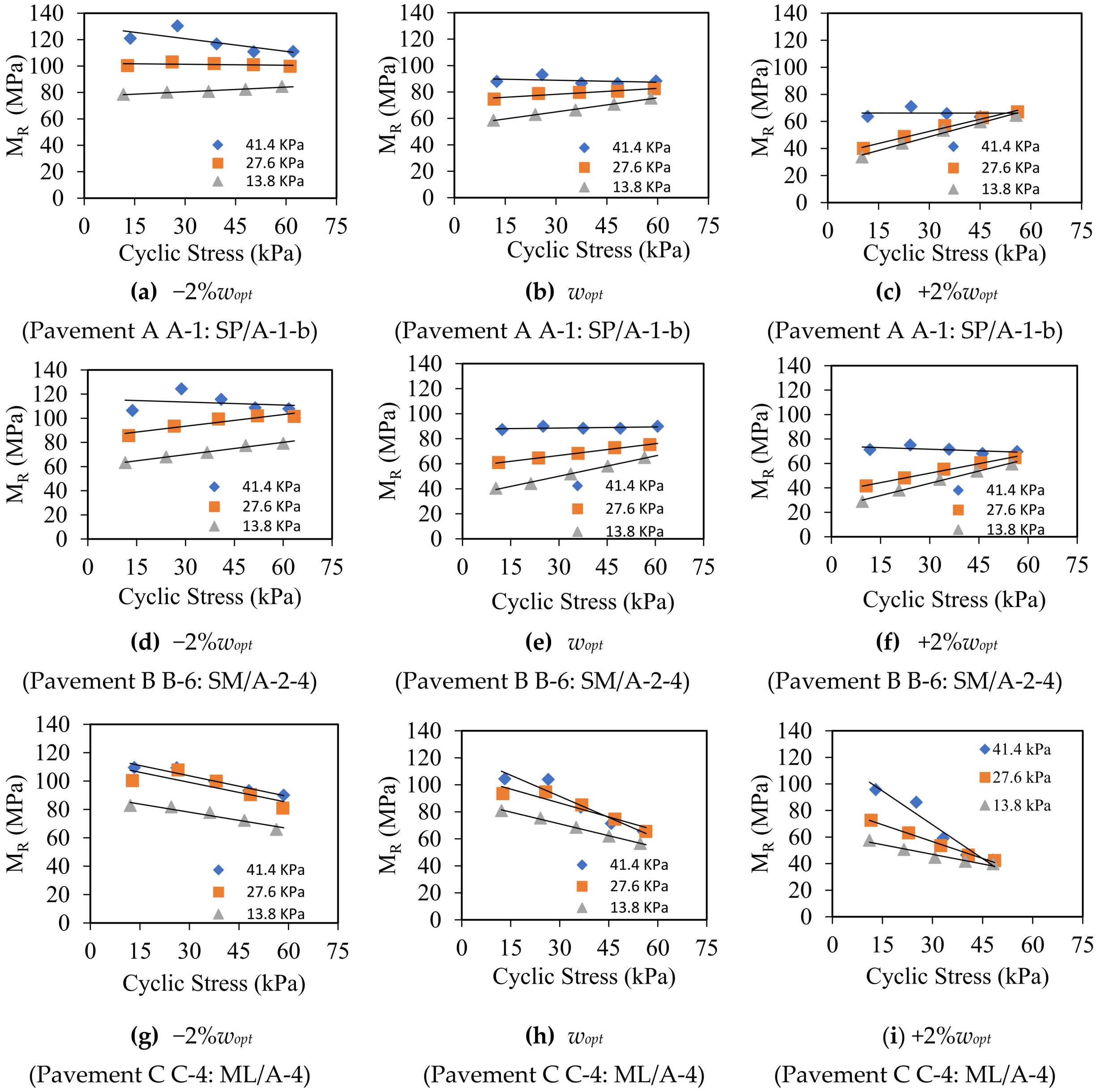

(a) $-2\%w_{opt}$ (Pavement A A-1: SP/A-1-b)
(b) w_{opt} (Pavement A A-1: SP/A-1-b)
(c) $+2\%w_{opt}$ (Pavement A A-1: SP/A-1-b)
(d) $-2\%w_{opt}$ (Pavement B B-6: SM/A-2-4)
(e) w_{opt} (Pavement B B-6: SM/A-2-4)
(f) $+2\%w_{opt}$ (Pavement B B-6: SM/A-2-4)
(g) $-2\%w_{opt}$ (Pavement C C-4: ML/A-4)
(h) w_{opt} (Pavement C C-4: ML/A-4)
(i) $+2\%w_{opt}$ (Pavement C C-4: ML/A-4)

Figure 3. Resilient Modulus Test Results.

Furthermore, as the moisture content increases from $-2\%w_{opt}$ to w_{opt} to $+2\%w_{opt}$, M_R decreases for each cyclic stress and confining pressure. Hence, tests performed on specimens compacted on the dry side of optimum showed higher M_R than those compacted at w_{opt}, and those compacted on the wet side of optimum showed lower M_R than those compacted at w_{opt}. Moreover, M_R for the specimens compacted on the wet side of optimum are less sensitive to the confining pressure at higher cyclic stress.

4.4. M_R Model Parameters and the Effects of Moisture Content

Model parameters were obtained for the generalized constitutive resilient modulus model used in the AASHTO M-E Pavement Design Guide (Equation (1)). Table 3 shows three states (dry, optimum, and wet) for 24 samples. Most of the test results show a good coefficient of determination ($R^2 > 0.80$). Results indicate that for the eight soil types, specimens prepared on the dry side of w_{opt} have a higher M_R than those prepared at w_{opt}, and those prepared at w_{opt} have a higher M_R than those prepared on the wet side of w_{opt}. In general, as shown in Figure 4, as the moisture increases, M_R decreases for all soils tested herein, as observed by others (e.g., refs. [28,47–51]). In most cases, the dry densities of the specimens compacted at w_{opt} are close to those compacted at $\pm 2\% w_{opt}$ (see Table 3). Thus, for small changes in density, i.e., 19.35 kN/m^3 and 19.57 kN/m^3 for specimens compacted at $-2\% w_{opt}$ and w_{opt} respectively for Pavement B B-3, there is no clear trend in M_R.

Table 3. Resilient Modulus Model Parameters.

Site	Soil	State	γ_d (kN/m^3)	MC (%)	k_1	k_2	k_3	R^2	M_R (MPa)
Pavement A	A-1 (SP/A-1-b)	Dry	19.01	7.8	1134	0.5054	−1.3099	0.97	121
		w_{opt}	19.26	9.5	777	0.3886	−0.3628	0.96	89
		Wet	18.74	11.2	449	0.3814	1.2511	0.79	62
	A-4 (SP/A-3)	Dry	17.04	10.3	830	0.4098	0.5921	0.99	107
		w_{opt}	17.12	11.9	763	0.5265	0.4989	0.99	103
		Wet	16.37	13.7	694	0.4645	0.4067	0.99	90
Pavement B	B-3 (SC/A-2-4)	Dry	19.35	8.5	1219	0.5585	−1.8260	0.92	125
		w_{opt}	19.57	10.2	617	0.5820	−1.7710	0.70	65
		Wet	18.60	12.0	303	0.2642	1.6491	0.63	42
	B-6 (SM/A-2-4)	Dry	18.49	7.0	955	0.6050	−0.7623	0.96	114
		w_{opt}	19.04	8.9	667	0.7167	−0.4379	0.97	87
		Wet	18.68	10.5	480	0.6250	0.5291	0.86	68
	B-8 (SC-SM/A-2-4)	Dry	19.45	8.0	879	0.8272	−2.1703	0.96	97
		w_{opt}	19.56	9.3	617	0.6108	−0.1492	0.82	79
		Wet	18.14	11.9	188	0.7616	−0.1470	0.81	26
Pavement C	C-2 (SM/A-7-6)	Dry	17.45	13.2	1047	0.4518	−3.0797	0.95	89
		w_{opt}	17.72	14.7	1147	0.4173	−4.4504	0.94	81
		Wet	17.39	16.7	292	0.4084	−4.7921	0.67	20
	C-4 (ML/A-4)	Dry	15.39	16.9	1183	0.3862	−2.1402	0.87	109
		w_{opt}	16.24	18.1	1192	0.3151	−3.1520	0.90	94
		Wet	16.21	19.8	1037	0.4409	−5.1491	0.90	68
	C-5 (SC/A-7-6)	Dry	18.25	11.2	1288	0.3607	−1.8520	0.85	122
		w_{opt}	18.46	13.2	1093	0.6480	−5.4391	0.94	76
		Wet	18.08	14.3	389	0.6976	−6.1519	0.87	25

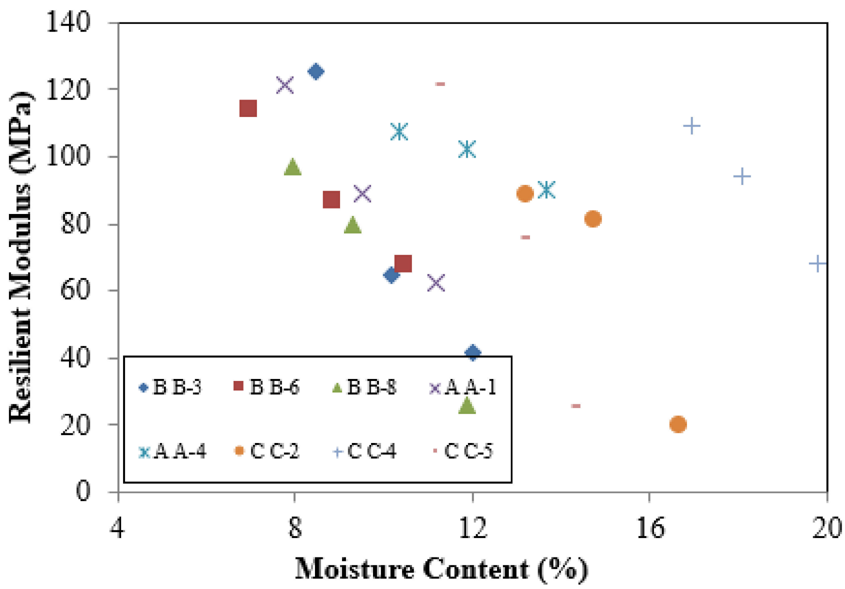

Figure 4. Effects of Moisture Content with Resilient Modulus.

4.5. Correlation of Resilient Modulus with CBR Values

Correlations between M_R and CBR are shown in Figure 5. Figure 5a shows the correlation between M_R and CBR for both 2.54 mm and 5.08 mm penetration and indicates that CBR increases with increasing M_R for both penetrations, with the M_R for 2.54 mm penetration being approximately 6% higher than 5.08 mm penetration. Figure 5b shows the correlation between M_R and CBR as a function of different soil types and indicates that CBR increases with increasing M_R for all soils tested herein. The following correlation Equation (3) between M_R and CBR was developed for South Carolina using the CBR data for all 24 samples at 2.54 mm penetration:

$$M_R(\text{MPa}) = 35.7 \times \text{CBR}^{0.35} \tag{3}$$

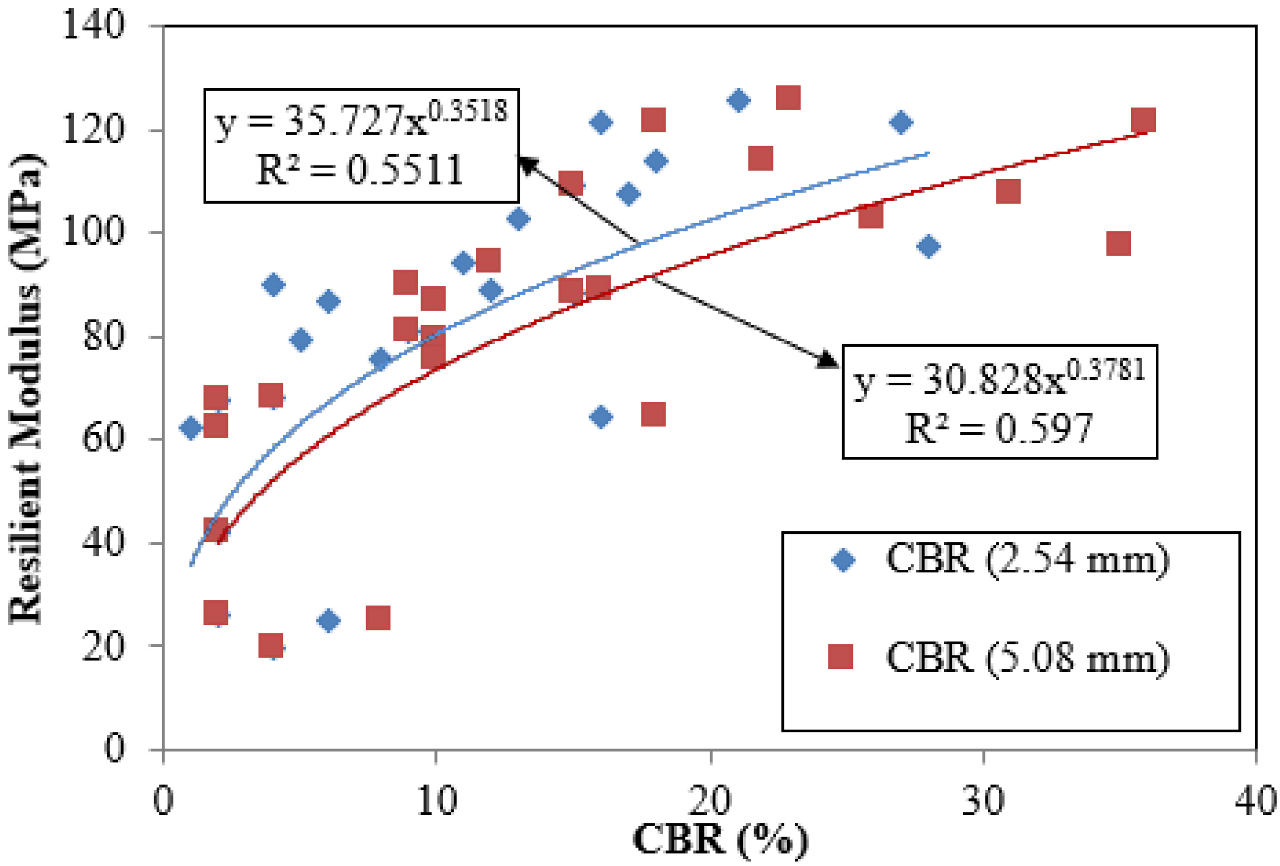

(a) Resilient Modulus vs. CBR for Different Penetrations

Figure 5. *Cont.*

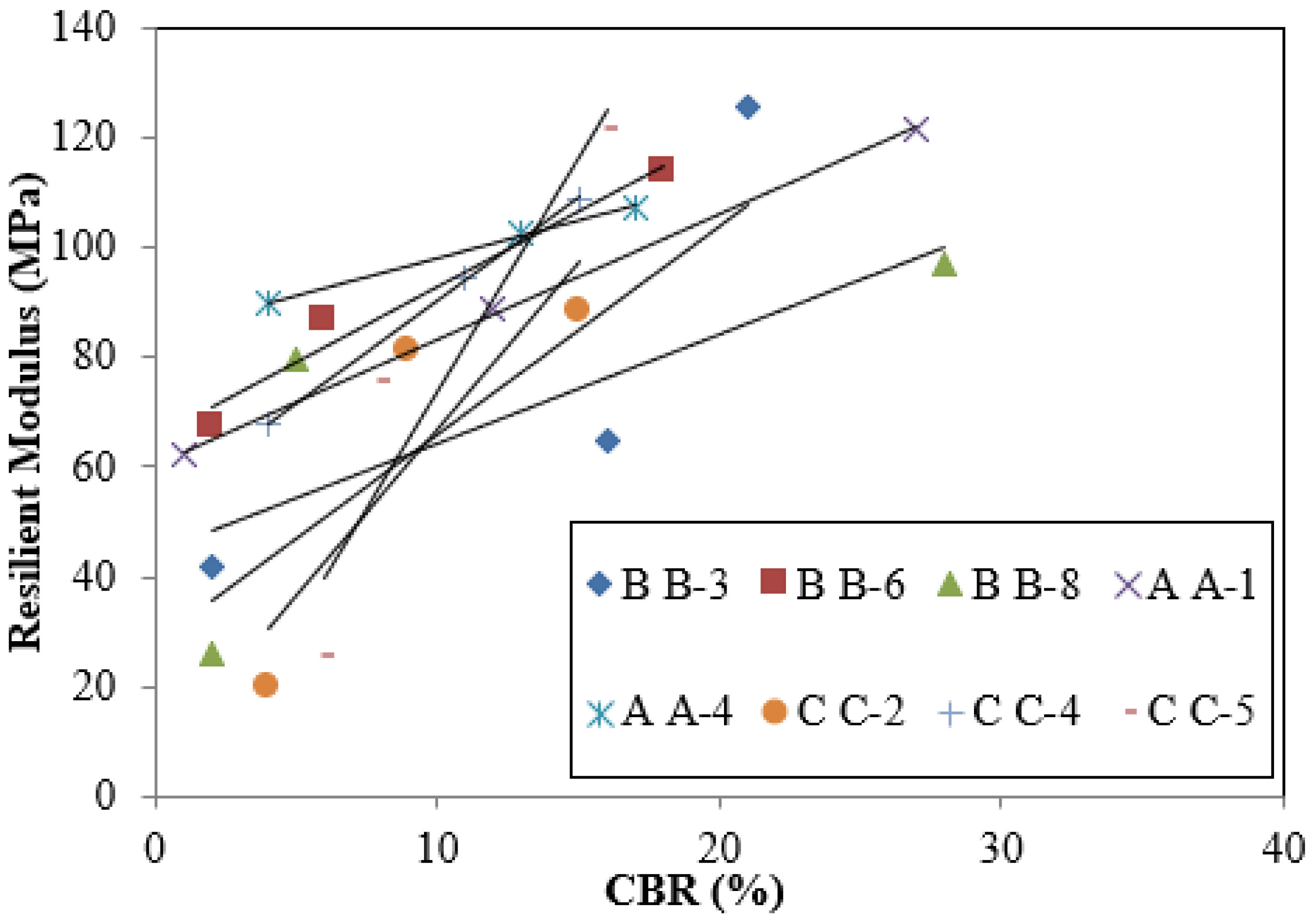

(b) Resilient Modulus vs. CBR for Different Soils

Figure 5. Resilient Modulus with CBR.

4.6. Correlation of Laboratory-Measured Resilient Modulus and M_R Obtained from Falling Weight Deflectometer

Figure 6 compares the average laboratory-measured M_R for all samples tested at the three sites ($-2\%w_{opt}$, w_{opt}, and $+2\%w_{opt}$) and FWD back-calculated M_R results. Generally, higher M_R was observed for the sites with coarse-grained soils (Pavement A and Pavement B). The average laboratory $M_{R(Lab)}$ was 70–80% less for these sites than the $M_{R(FWD)}$. For the site with fine-grained soils (Pavement C), the laboratory $M_{R(Lab)}$ was approximately 60% less than the $M_{R(FWD)}$. Higher FWD values can be obtained from different FWD equipment, loading magnitudes, or back-calculation tools [50]. Johnson (1992) [51] developed a correlation between FWD-derived modulus and laboratory-resilient modulus. He found that the maximum ratio of $M_{R(FWD)}$ to $M_{R(Lab)}$ is 12.4, the minimum ratio is 1.8, and the average ratio for all sites is 5.7. Table 4 shows the C factors found for coarse and fine-grained soils at each of $-2\%w_{opt}$, w_{opt}, and $+2\%w_{opt}$. Table 4 also lists the combined C value for coarse and fine-grained soils. Results showed that the C values are influenced by the moisture content. The correlation between the FWD back-calculated modulus and the laboratory M_R developed here is shown in Equation (4) and used to find the coefficient of conversion (C-factor) in the relation (see Equation (4)):

$$M_{R(FWD)}\ (\text{MPa}) = C \times M_{R(Lab)} \quad (4)$$

where C = 3.6 for coarse and fine-grained soils.

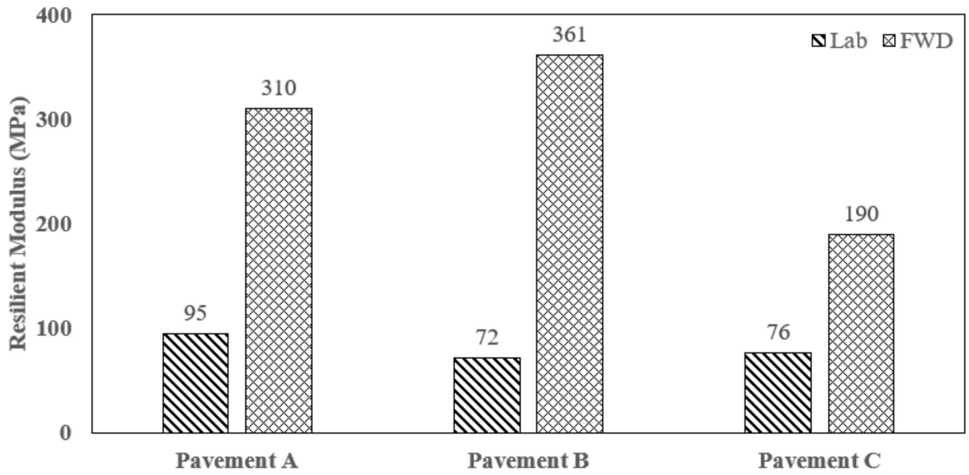

Figure 6. Relationship between Laboratory and Backcalculated FWD M_R.

Table 4. Developed C factors for Coarse and Fine-Grained Soil Samples.

Moisture Condition	Coarse-Grained Soils		Fine-Grained Soils		Combined Coarse and Fine-Grained Soils	
	C^1	C^2	C^1	C^2	C^1	C^2
$-2\%w_{opt}$	0.33	3.06	0.30	3.38	0.30	3.6
w_{opt}	0.25	3.97	0.23	4.31		
$2\%w_{opt}$	0.17	5.82	0.10	9.58		

C^1 factor w respect to $M_{R(Lab)}$ to $M_{R(FWD)}$; C^2 factor w respect to $M_{R(FWD)}$ to $M_{R(Lab)}$.

For pavement design consideration, the laboratory-measured $M_{R(Lab)}$ using the NCHRP 285 [39] stress conditions are more conservative than the backcalculated $M_{R(FWD)}$. It is recommended that state agencies develop an M_R design catalog for using local soils as input Level 2 during flexible pavement design. Proper selection of the subgrade resilient modulus can significantly affect the required thicknesses of the pavement layers and directly influence the cost. There are no unique methods to back-calculate the M_R from FWD data. Different back-calculation tools give different values. Islam et al. (2020) [52] found that the average M_R for the BAKFAA and AASHTOWare tools are around 6% different. In contrast, the average M_R along the pavement length found using the SCDOT program was approximately 21–30 % lower than the other two tools. Furthermore, seasonal variation, climate, temperature, and surface condition of the asphalt concrete layer affect the deflection data of the FWD test [51–54].

4.7. Correlation of Resilient Modulus Model Parameters with Soil Index Properties

Using multiple linear regression techniques, the generalized constitutive resilient modulus model parameters (k_1, k_2, and k_3) for remolded soils were correlated with soil index properties. The soil properties considered in the statistical analysis include the compacted soil dry density (γ_d), moisture content (w), maximum dry density ($\gamma_{d,\ max}$), optimum moisture content (w_{opt}), percent passing through No. 4 (P_4), No. 40 (P_{40}), and No. 200 sieve (P_{200}), D_{60}, D_{50}, D_{30}, D_{10}, uniformity coefficient (C_u), coefficient of curvature (C_c), liquid limit, plastic limit, plasticity index (PI), liquidity index (LI), specific gravity (G_s), and the percent of sand, silt, and clay. Combined statistical models were developed using the results for the eight soils. Table 5 shows the coefficients for the developed models. Coefficients of determination (R^2) of 0.43, 0.61, and 0.71 were found for k_1, k_2, and k_3, respectively.

Table 5. Developed Constitutive Models of Coefficients.

Models	R^2	F Value
$k_1 = -25340.939^{**} + 238.99P_4\ ^{**} - 43.411LI + 12.77\left(w_{opt} \times \gamma_{d,max}\right)\ ^{***}$ $-92.557\left(\gamma_{d,max}\right)^{**} + 559.692\left(\frac{w}{w_{opt}} \times \frac{\gamma_d}{\gamma_{d,max}}\right)$	0.43	3.58 *
$k_2 = +9.958\ ^{**}\ -0.075P_4\ ^{*} + 0.037LI\ ^{***} - 0.002\left(w_{opt} \times \gamma_{d,max}\right)^{**} - 0.635\left(\frac{w}{w_{opt}} \times \frac{\gamma_d}{\gamma_{d,max}}\right)^{***}$ $-0.613(G_s)\ ^{*} + 0.839\left(\frac{\gamma_d}{\gamma_{d,max}}\right)\ ^{*}$ -0.078	0.61	6.06 ***
$k_3 = -63.2 + 0.682P_4{}^{*} - 0.235LI^{**} - 0.03\left(w_{opt} \times \gamma_{d,max}\right)^{***}$	0.71	21.01 ***

* $p < 0.05$; ** $p < 0.01$; *** $p < 0.001$.

Table 5 shows the significance of different soil properties on the coefficients and overall model significance using p-value, where $p < 0.001$ indicates a statistically significant effect. $p < 0.01$ and $p < 0.05$ indicate statistically moderate and low significant effects, respectively. For the eight soils tested, P_4, LI, w_{opt}, and $\gamma_{d,max}$ showed a statistically significant effect on all three model coefficients (k_1, k_2, and k_3); w and γ_d showed a statistically significant effect on k_1 and w, γ_d, and G_s showed a statistically significant effect on k_2.

Predicted and measured k_1, k_2, k_3 are shown in Figure 7a–c, respectively. Model coefficients k_1, k_2, and k_3 are the regression constants of Equation (1). Therefore, these were measured from the applied bulk stresses and octahedral shear stresses. The resultant resilient modulus values were obtained from 15 test sequences using regression analysis for each test. Most of the data points for all three models are observed close to the equity line.

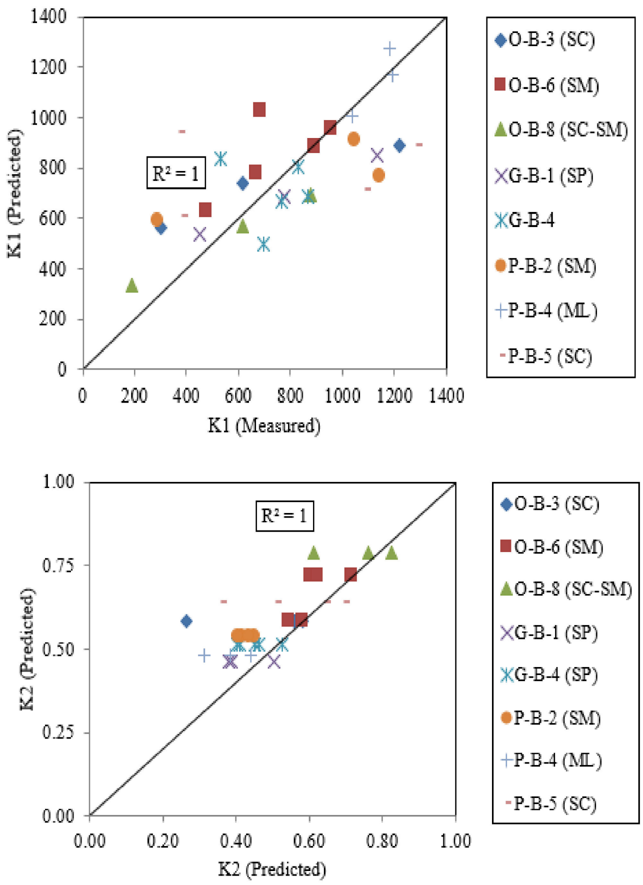

Figure 7. *Cont.*

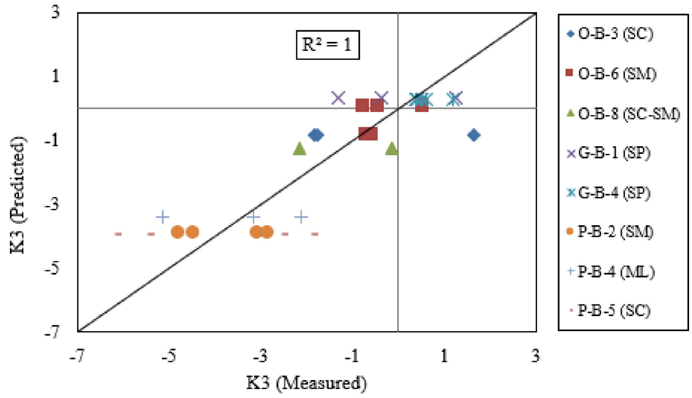

Figure 7. Predicted versus Measured Model Coefficients.

The laboratory-measured $M_{R(Lab)}$ is compared to the predicted M_R in Figure 8a and to the LTPP sand model in Figure 8b. The predicted M_R (from the locally developed constitutive model) more accurately predicted M_R than the LTPP sand model in terms of lower bias (e.g., −2.07 vs. 37.40) and standard error (SE) (e.g., 21.56 vs. 34.59). The LTPP model for silts and the LTPP model for clay were also studied. However, the LTPP model for sand showed better results when compared to the measured M_R for the soils studied herein. These results demonstrate the importance of performing local calibration studies to find the constitutive model parameters for use in the MEPDG rather than using the universal constitutive model parameters found within the LTPP program [52].

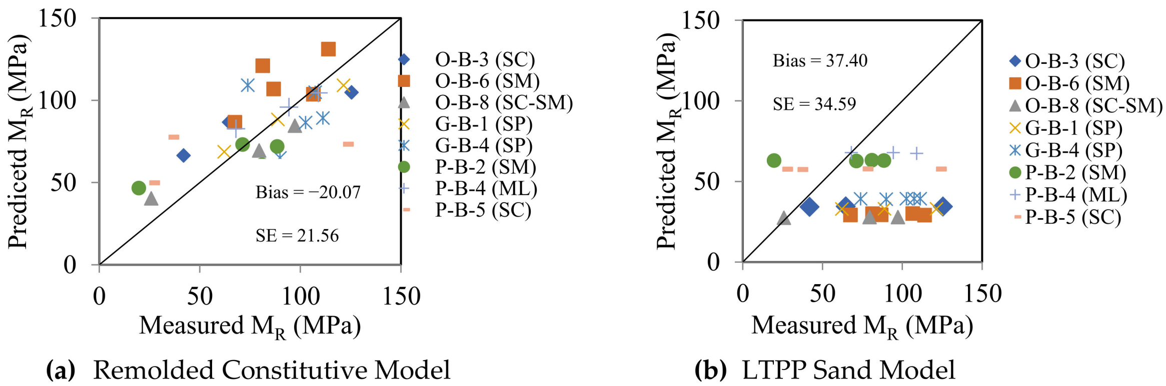

Figure 8. Comparison of Different Models.

5. Effect of Subgrade Resilient Modulus on Pavement Rutting

Figure 9 shows the cumulative rutting of different layers for each of the three pavement sections. Rutting for the AC layer only, rutting for the AC and base layer, and total rutting (AC + base + subgrade rutting) are shown. Pavement rutting is shown for five different subgrades M_R inputs ($M_{R(Lab,\ Dry)}$, $M_{R(Lab,\ w_{opt})}$, $M_{R(Lab,\ Wet)}$, $M_{R(FWD)}$, and $M_{R(Default)}$) to show the effect of subgrade moisture content and the influence of M_R for designing flexible pavement. For all three sites, the highest total rutting was obtained using an M_R wet of optimum as the input for the subgrade soil, and the lowest total rutting was obtained using an $M_{R(FWD)}$.

For Pavement A (Figure 9a) showed subgrade rutting of 8.58, 7.75, and 7.23 mm, respectively, for the $M_{R(Lab,\ Wet)}$, $M_{R(Lab,\ w_{opt})}$, and $M_{R(Lab,\ Dry)}$, respectively, a pavement age of 20 years. Pavement A also follows a similar trend to Pavement B, but the total rutting is approximately 2 times greater. The predicted total rutting using $M_{R(FWD)}$ is lower than other inputs except for AC and AC+Base layer conditions.

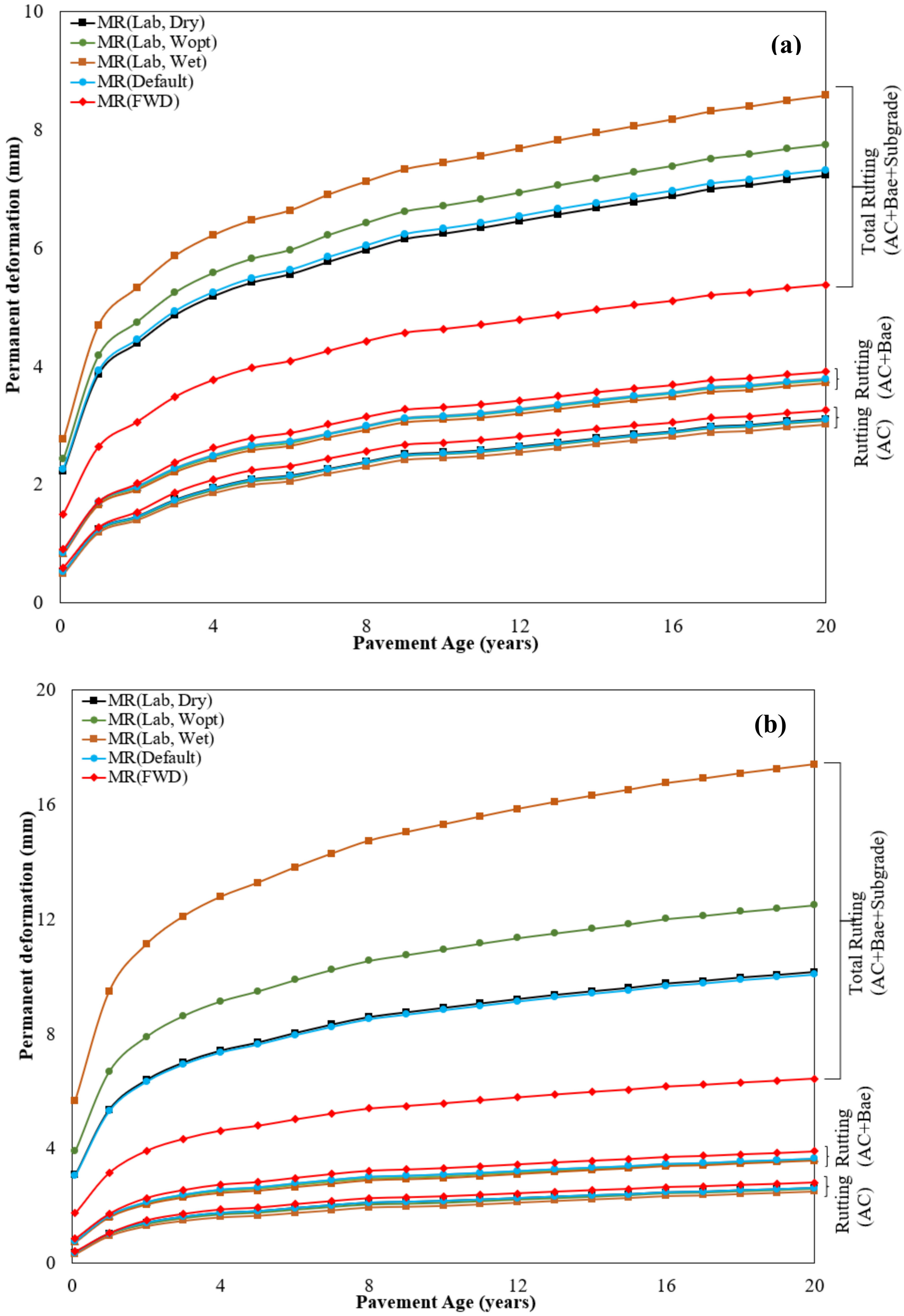

Figure 9. *Cont.*

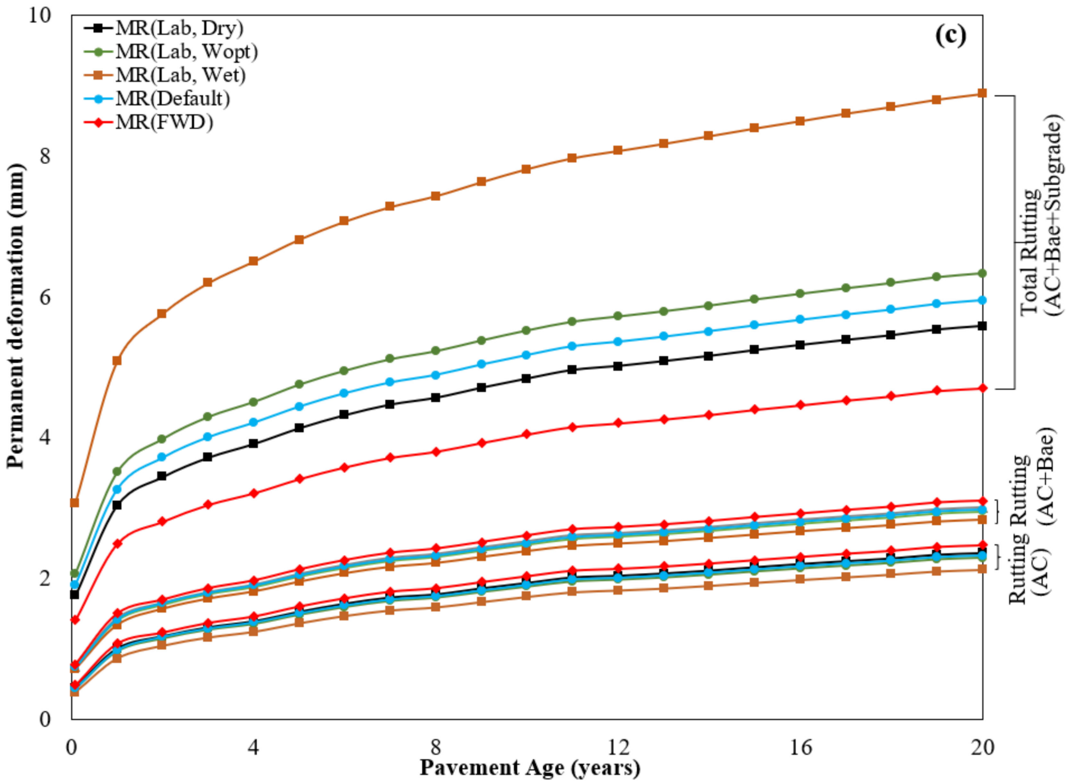

Figure 9. Effects of Subgrade M_R on Pavement Rutting: (**a**) Pavement A, (**b**) Pavement B, and (**c**) Pavement C.

As observed for Pavement B in Figure 9b, using a wet of optimum $M_{R(Lab,\, w_{opt})}$, as the input for the subgrade soil showed subgrade rutting (total rutting—AC and base rutting) that is approximately 1.7 times the subgrade rutting using a dry of optimum $M_{R(Lab,\, Dry)}$, for a pavement age of 20 years (17.41 mm versus 10.15 mm subgrade rutting). Using the $M_{R(Lab,\, w_{opt})}$, found at w_{opt} produced rutting that was in between these values (7.26 mm). That means it indicates higher moisture content produced lower subgrade M_R and predicts the total pavement rutting. The figure also shows that the $M_{R(FWD)}$ predicted higher rutting (AC layer only, and AC and base layer) than laboratory-measured $M_{R(Lab)}$. It can be observed that subgrade M_R directly influences the total pavement rutting. The $M_{R(Default)}$ predicts approximately 1.5 times higher total rutting than the $M_{R(FWD)}$ and is also close to the dry side of optimum $M_{R(Lab,\, Dry)}$.

Pavement C showed the largest subgrade rutting (8.88 mm) for the $M_{R(Lab,\, Wet)}$ at wet of optimum (Figure 9c). Even though Pavement B has a higher subgrade $M_{R(Lab,\, Wet)}$ for the wet side of optimum (45 MPa) than that of Pavement C (38 MPa), higher subgrade rutting (12.5 n Pavement B) was observed (6.33 mm in Pavement C). This is because subgrade rutting is affected by the rutting of the layers above it (i.e., base layer rutting and AC rutting). These three sites were modeled with the same AC layer but a different type of base layer: Pavement A has a 152.2 mm thick cement stabilized aggregate base (CSB), Pavement B has a 152.2 mm thick graded aggregate base (GAB), and Pavement C has a 147.3 mm thick asphalt treated aggregate base (AAB) (see Table 5).

The GAB has a lower modulus (E = 138 MPa) than CSB and AAB (E = 6894 MPa); therefore, the largest subgrade rutting (and total rutting) was observed for all three M_R inputs (wet, w_{opt}, dry) for the Pavement B site with GAB as the base course (see Figure 9b) when compared to the Pavement A and Pavement C sections with CSB and AAB as the base courses (see Figure 9b,c), respectively. This indicates that the effect of moisture variation on the M_R for a subgrade layer, and the resulting rutting predicted in MEDPG, is more important when an untreated unbound layer (i.e., GAB) is present than when a stabilized layer (i.e., cement stabilized aggregate base layer or asphalt aggregate base layer) is present.

Overall, laboratory-measured M_R (wet, w_{opt}, dry) predicts higher total pavement rutting than back-calculated $M_{R(FWD)}$ and $M_{R(default)}$ obtained from soil classification except for Pavement C. According to AASHTOWare Pavement ME Design software (version 2.6.1), both M_R values are classified as Level 2 input parameters for subgrade resilient modulus. The default M_R values (Level 3) are inconsistent in predicting pavement rutting. Sometimes, it showed that the expected pavement rutting was in close agreement with the dry side of M_R (~1% difference) (see Figure 9a,b), and sometimes it exhibited more than a 6% difference (See Figure 9c). The default $M_{R(default)}$ exhibits higher total rutting than the dry side of optimum $M_{R(Lab,\ Dry)}$ for a pavement age of 20 years (5.95 mm versus 5.58 mm subgrade rutting) at the Pavement C site.

6. Conclusions

This paper presented an extensive field and laboratory testing program to establish subgrade material input parameters for predicting rutting over 20 years using MEPDG. FWD tests were performed along three asphalt concrete pavement sections, e.g., Pavement A, Pavement B, and Pavement C, and the AASHTOWare back-calculation tool [41] was used to backcalculate $M_{R(FWD)}$. Standardized field and laboratory methods were used to collect natural subgrade samples and characterize $M_{R(Lab)}$ through repeated load triaxial tests per AASHTO T 307. Multiple linear regression techniques were used to establish the generalized constitutive resilient modulus model parameters ($k_1,\ k_2,\ and\ k_3$) for remolded soils and were correlated with soil index properties. Correlations were developed between $M_{R(Lab)}$ vs. $M_{R(FWD)}$ and $M_{R(Lab)}$ vs. CBR. Based on the analysis, the following conclusions can be drawn:

- The peak value of both CBR and $M_{R(Lab)}$ was found on the dry side of w_{opt} and at a γ_d less than the maximum.
- $M_{R(Lab)}$ decreases as the moisture content increases. Specimens compacted at $-2\%w_{opt}$ showed higher $M_{R(Lab)}$ than specimens compacted at w_{opt}. Specimens compacted at $+2\%w_{opt}$ showed lower $M_{R(Lab)}$ than specimens compacted at w_{opt}.
- The resilient modulus for the specimens compacted on the wet side of w_{opt} is less sensitive to the confining pressure at higher cyclic stress.
- A good correlation was made between $M_{R(Lab)}$ and CBR. $M_{R(Lab)}$ increases with increasing CBR for the different soils.
- Percent passing the No. 4 sieve, liquidity index, optimum moisture content, and maximum dry density showed a statistically significant effect on the coefficients of the generalized constitutive resilient modulus model.
- The locally developed constitutive models of coefficients predicted M_R more accurately than the universal LTPP models in lower bias and standard error.
- Back-calculated $M_{R(FWD)}$ is approximately 3.6 times higher than laboratory-measured $M_{R(Lab)}$ using the NCRHP 285 stress state [34]. The value of the C factor is influenced by moisture content (see Table 4). Future work using the in-situ stress state is warranted.
- Laboratory-measured $M_{R(Lab)}$ predicted higher pavement rutting compared to FWD.
- If a graded aggregate base is used, the soil moisture condition significantly influences the subgrade M_R and the resulting subgrade rutting. However, if a higher stiffness base layer is used (i.e., cement-stabilized base or asphalt-treated aggregate base), the moisture effect is less significant.

Author Contributions: Conceptualization, methodology, software, validation, writing—original draft, writing-review and editing, M.M.R.; conceptualization, methodology, writing—review and editing, S.L.G.; conceptualization, methodology, software, writing—review and editing, K.M.I. All authors have read and agreed to the published version of the manuscript.

Funding: This project was funded by the SCDOT and the FHWA [grant SPR 708]. Any opinions, findings, conclusions, or recommendations expressed in this material are those of the authors and do not necessarily reflect the views of the SCDOT or the FHWA.

Data Availability Statement: Not applicable.

Acknowledgments: The writers would like to acknowledge the SCDOT for the sponsorship of this project. The opinions, findings and conclusions expressed herein are those of the authors and not necessarily those of the SCDOT or FHWA. The authors would like to express gratitude to USC graduate students Emad Gheibi and M. Majbah Uddin for their assistance in the soil index tests and statistical analyses. The authors would also like to express gratitude to USC undergraduate students Lex Nelson and Javonte Isaac or performing Atterberg limit tests for this study.

Conflicts of Interest: The authors declare no conflict of interest.

References

1. Zaghloul, S.; Ayed, A.; Halim, A.A.; Vitillo, N.; Sauber, R. Investigations of Environmental and Traffic Impacts on Mechanistic-Empirical Pavement Design Guide Predictions. *Transp. Res. Rec.* **2006**, *1967*, 148–159. [CrossRef]
2. Jadoun, F.M.; Kim, Y.R. Calibrating Mechanistic-Empirical Pavement Design Guide for North Carolina. *Transp. Res. Rec.* **2012**, *2305*, 131–140. [CrossRef]
3. Zapata, C.E.; Andrei, D.; Witczak, M.W.; Houston, W.N. Incorporation of Environmental Effects in Pavement Design. *Transp. Res. Rec.* **2007**, *8*, 667–693. [CrossRef]
4. Johanneck, L.; Khazanovich, L. Comprehensive Evaluation of Effect of Climate in Mechanistic–Empirical Pavement Design GuidePredictions. *Transp. Res. Rec. J. Transp. Res. Board* **2010**, *2170*, 45–55. [CrossRef]
5. Saxena, P.; Tompkins, D.; Khazanovich, L.; Balbo, T. Evaluation of Characterization and Performance Modeling of Cementitiously Stabilized Layers in the Mechanistic-Empirical Pavement Design Guide. *Transp. Res. Rec.* **2010**, *2186*, 111–119. [CrossRef]
6. Hossain, Z.; Zaman, M.; Doiron, C.; Solanki, P. Evaluation of Mechanistic-Empirical Design Guide Input Parameters for Resilient Modulus of Subgrade Soils in Oklahoma. *J. Test. Eval.* **2011**, *39*, 803–814.
7. Singh, D.; Zaman, M.; Commuri, S. Evaluation of Measured and Estimated Dynamic Moduli for Selected Asphalt Mixed. *J. ASTM Int.* **2011**, *8*, 1–19.
8. Xu, Q.; Ruiz, M.; Moravec, M.; Rasmussen, R.O. Simulation of Unbound Material Resilient Modulus Effects on Mechanistic-Empirical Pavement Designs. *Mater. Struct.* **2013**, *46*, 1089–1100. [CrossRef]
9. American Association of State Highway and Transportation Officials (AASHTO). *Mechanistic-Empirical Pavement Design Guide: A Manual of Practice, Interim Edition*; AASHTO: Washington, DC, USA, 2008.
10. Orobio, A.; Zaniewski, J.P. Sampling-Based Sensitivity Analysis of the Mechanistic–Empirical Pavement Design Guide Applied to Material Inputs. *Transp. Res. Rec. J. Transp. Res. Board* **2011**, *2226*, 85–93. [CrossRef]
11. Islam, K.M.; Gassman, S.L. Predicting Flexible Pavement Distress and IRI Considering Subgrade Resilient Modulus of Fine-Grained Soils Using MEPDG. *Materials* **2023**, *16*, 1126. [CrossRef]
12. Ksaibati, K.; Armaghani, J.; Fisher, J. Effect of Moisture on Modulus Values of Base and Subgrade Materials. *Transp. Res. Rec. J. Transp. Res. Board* **2000**, *1716*, 20–29. [CrossRef]
13. Flintsch, G.W.; Al-Qadi, I.L.; Park, Y.; Brandon, T.L.; Appea, A. Relation between Back-calculated and Laboratory Measured Resilient Modulus of Unbound Materials. *Transp. Res. Rec.* **2003**, *1849*, 1177–1182. [CrossRef]
14. Nazzal, M.D.; Mohammad, L.N. Estimation of Modulus Resilient of Subgrade Soils using Falling Weight Deflectometer. *Transp. Res. Rec.* **2010**, *2186*, 1–10. [CrossRef]
15. Islam, K.M.; Gassman, S.; Rahman, M.M. Field and laboratory characterization of subgrade resilient modulus for pavement mechanistic-empirical pavement design guide application. *Transp. Res. Rec.* **2020**, *2674*, 921–930. [CrossRef]
16. Islam, K.M.; Gassman, S.L. Estimation of Subgrade Modulus Using Falling Weight Deflectometer. In *Tran-SET 2021*; American Society of Civil Engineers: Reston, VA, USA, 2021; pp. 247–258. [CrossRef]
17. Islam, K.M.; Gassman, S.L. Influence of Subgrade Resilient Modulus Selection Methodology on AASHTOWare Pavement ME Design. *Geo-Congress* **2022**, 192–204. [CrossRef]
18. Chen, D.; Wang, J.; Bilyeu, J. Application of Dynamic Cone Penetrometer in Evaluation of Base and Subgrade Layers. *Transp. Res. Rec.* **2001**, *1764*, 1–10. [CrossRef]
19. Heukelom, W.; Klomp, A.J.G. Dynamic Testing as a Means of Controlling Pavement during and after Construction. In Proceedings of the 1st International Conference on the Structural Design of Asphalt Pavement, Ann Arbor, MI, USA, 20–24 August 1962; University of Michigan: Ann Arbor, MI, USA, 1962.
20. George, K.P. *Prediction of Resilient Modulus from Soil Properties Publication FHWA-MS-04-172, F.H.W.A.*; US Department of Transportation: Washington, DC, USA, 2004.
21. Garg, N.; Larkin, A.; Brar, H. A Comparative Subgrade Evaluation using CBR, Vane Shear, Light Weight Deflectometer, and Resilient Modulus Tests. In Proceedings of the 8th International Conference on the Bearing Capacity of Roads, Railways and Airfields, Champaign, IL, USA, 29 June–2 July 2009; Volume 5, pp. 57–64.
22. Yau, A.; Von Quintus, H.L. Predicting Elastic Response Characteristics of Unbound Materials and Soils. *Transp. Res. Rec.* **2004**, *1874*, 47–56. [CrossRef]
23. Kim, D.; Kim, J.R. Resilient Behavior of Compacted Subgrade Soils Under the Repeated Triaxial Test. *Constr. Build. Mater.* **2007**, *21*, 1470–1479. [CrossRef]

24. Malla, R.B.; Joshi, S. Resilient Modulus Prediction Models Based on Analysis of LTPP Data for Subgrade Soils and Experimental Verifications. *Int. J. Transp. Eng.* **2007**, *133*, 491–504. [CrossRef]
25. Zhou, C.; Huang, B.; Drumm, E.; Xiang, S.; Qiao, D.; Udeh, S. Soil Resilient Modulus Regressed from Physical Properties and Influence of Seasonal Variation on Asphalt Pavement Performance. *J. Transp. Eng.* **2014**, *141*, 1–9. [CrossRef]
26. Titi, H.H.; English, R.; Faheem, A. Resilient Modulus of Fine-Grained Soils for Mechanistic-Empirical Pavement Design. *Transp. Res. Rec.* **2015**, *2510*, 24–35. [CrossRef]
27. Guan, Y.; Drumm, E.C.; Jackson, N.M. Weighting Factor for Seasonal Subgrade Resilient Modulus. *Transp. Res. Rec.* **1998**, *1821*, 47–55. [CrossRef]
28. Heydinger, A.G. Evaluation of Seasonal Effects on Subgrade Soils. *Transp. Res. Rec.* **2003**, *1619*, 94–101. [CrossRef]
29. Khoury, N.N.; Zaman, M.M. Correlation Between Resilient Modulus, Moisture Variation, and Soil Suction for Subgrade Soils. *Transp. Res. Rec.* **2004**, *1874*, 99–107. [CrossRef]
30. Ceratti, J.A.; Gehling, W.Y.; Nunez, W. Seasonal Variation of a Subgrade Soil Resilient Modulus in Southern Brazil. *Transp. Res. Rec.* **2004**, *1876*, 165–173. [CrossRef]
31. Puppala, A.J.; Saride, S.; Chomtid, S. Experimental and Modeling Studies of Permanent Strains of Subgrade Soils. *J. Geotech. Geoenvironmental Eng.* **2009**, *135*, 1379–1389. [CrossRef]
32. Hicks, R.G.; Monismith, C.L. *Factors Influencing the Resilient Properties of Granular Materials, Transportation Research Record 345, Transportation Research Board*; National Research Council: Washington, DC, USA, 1971; pp. 15–31.
33. Taheri, A.; Tatsuoka, F. Primary stress–strain relations inferred from multiple-step triaxial compression test results. *Soils Found* **2012**, *52*, 748–766. [CrossRef]
34. De Freitas, J.B.; de Rezende, L.R.; de F.N. Gitirana, G., Jr. Prediction of the resilient modulus of two tropical subgrade soils considering unsaturated conditions. *Eng. Geol.* **2020**, *270*, 105580. [CrossRef]
35. Perez-Garcia, N.; Fredlund, D.; Garnica-Anguas, P.; Mestas-Martinez, N. A model to predict changes in resilient modulus resulting from wetting and drying. *Infraestruct. Vial* **2015**, *17*, 23–30. [CrossRef]
36. Khoury, N.; Brooks, R.; Khoury, C. Environmental influences on the engineering behavior of unsaturated undisturbed subgrade soils: Effect of soil suctions on resilient modulus. *Int. J. Geotech. Eng.* **2009**, *3*, 303–311. [CrossRef]
37. *AASHTO T 193*; Standard Test Method of Test for the California Bearing Ratio Test. Standard Specifications for Transportation Materials and Methods of Sampling and Testing. AASHTO: Washington, DC, USA, 2003.
38. *AASHTO-T307-99*; Standard Method of Test for Determining the Resilient Modulus of Soils and Aggregate Materials Standard Method of Test for Soils and Aggregate Materials. AASHTO: Washington, DC, USA, 2017.
39. *NCHRP 1-28A*; Laboratory Determination of Resilient Modulus for Flexible Pavement Design. National Cooperative Highway Research Program, Digest No. 285. AASHTO: Washington, DC, USA, 2004; pp. 1–52.
40. Dynatest Consulting, Inc. Dynatest FWD/HWD Test Systems. 2009. Available online: http://www.dynatest.com/media/4180/3_dynatest_fwd_hwd.pdf (accessed on 3 April 2022).
41. AASHTO ME Back-Calculation User Manual, User Manual for Pavement ME Deflection. Data Analysis and Back-Calculation Tool. 2017. Available online: https://me-design.com/MEDesign/data/BcT_UserManual.pdf (accessed on 7 February 2023).
42. Maher, A.; Bennert, T.; Gucunski, N. *Papp WJ Resilient Modulus Properties of New Jersey Subgrade Soils Publication FHWA-NJ-00-01, F.H.W.A.*; US Department of Transportation: Washington, DC, USA, 2000.
43. Ng, K.; Henrichs, Z.R.; Ksaibati, K.; Wulff, S.S. *Measurement and Estimation of the Resilient Modulus of Subgrade Materials for Mechanistic-Empirical Pavement Design Guide in Wyoming. Compendium of Papers of the 95th TRB Annual Meeting (CD-ROM)*; Transportation Research Board: Washington, DC, USA, 2016.
44. Gassman, S.L.; Rahman, M.M. *Calibration of the AASHTO Pavement Design Guide to South Carolina Conditions-Phase I*; FHWA-SC-16-02; US Department of Transportation: Washington, DC, USA, 2016.
45. Rahman, M.M.; Gassman, S.L. Data Collection Experience for Preliminary Calibration of the AASHTO Pavement Design Guide for Flexible Pavements in South Carolina. *Int. J. Pavement Res. Technol.* **2018**, *11*, 445–457. [CrossRef]
46. Rahman, M.M.; Gassman, S.L. Effect of Resilient Modulus of Undisturbed Subgrade Soils on Pavement Rutting. *Int. J. Geotech. Eng.* **2019**, *13*, 152–161. [CrossRef]
47. Fredlund, D.G.; Bergan, A.T.; Wong, P.K. Relation between Resilient Modulus and Stress Research Conditions for Cohesive Subgrade Soils. *Transp. Res. Rec.* **1977**, *642*, 73–81.
48. Drumm, E.C.; Reeves, J.S.; Madgett, M.R.; Trolinger, W.D. Subgrade Resilient Modulus Correction for Saturation Effects. *J. Geotech. Geo-Environ. Eng.* **1977**, *123*, 663–670. [CrossRef]
49. Butalia, T.S.; Huang, J.; Kim, D.G.; Croft, F. Effect of Moisture Content and Pore Water Pressure Build on Resilient Modulus of Cohesive Soils. In *Resilient Modulus Testing for Pavement Components, ASTM STP 1437*; ASTM International: West Conshohocken, PA, USA, 2003.
50. Tarefder, R.A.; Ahmed, M.U. Modeling of the FWD deflection basin to evaluate airport pavements. *Int. J. Geomech.* **2013**, *14*, 205–213. [CrossRef]
51. Johnson, A.M. Design of Flexible Pavement Overlays by Dynamic Deflections. Ph.D. Dissertation, University of South Carolina, Columbia, SC, USA, 1992.

52. Islam, K.M.; Rahman, M.M.; Gassman, S.L. Use of FWD Data to Subdivide Pavement Sections for MEPDG Calibration. In *Geo-Congress 2020: Geotechnical Earthquake Engineering and Special Topics*; American Society of Civil Engineers: Reston, VA, USA, 2020; pp. 426–435.
53. Lee, S.W.; Mahoney, J.P.; Jackson, N.C. Verification of Backcalculation of Pavement Moduli. *J. Transp. Res. Rec.* **1988**, *1196*, 131–135.
54. Hossain, M.; Romanoschi, S.; Gisi, A.J. Seasonal and Spatial Variations of Subgrade Response. *Geotech. Spec. Publ.* **2000**, *98*, 150–167.